

Thermal Model and Characteristics of Double Slope Solar Still

Rahul Dev¹ and Amimul Ahsan²

Submitted in August, 2013; Accepted in February, 2014

Abstract - In this paper, a new thermal model (after assuming temperatures of east and west side glass covers equal to their average temperature) and characteristics of double slope solar still (DSSS) have been developed. Experimental and theoretical results have been compared for the composite climate of New Delhi, India. Theoretical results obtained by previous and new thermal models of DSSS have been found in fair agreements with experimental observations. The characteristics have been developed under quasi-steady state of the solar still by linear and non-linear regression curves between daylight instantaneous gain/loss efficiencies and

$$\text{factor} \left\{ \frac{(T_{wEW} - T_a)}{(I_s(t)_E + I_s(t)_W)} \right\}.$$

Index Terms – Double slope solar still, Characteristic equation, Instantaneous efficiency, Thermal testing.

1.0 INTRODUCTION

Solar still is a solar energy operated water purification system. Researchers have developed several passive and active solar stills over the years [1-4]. Nebbia and Menozzi have mentioned Della Porta's solar still which was designed to extract the essence of herbs [5,6]. Dunkle [7] have developed correlations for various rates of heat and mass transfer of solar still. Similarly, Tsilingiris [8] have also developed temperature dependent correlations for internal heat transfer coefficients between water and glass cover of solar still and it was shown that these are affected adversely above 60 °C water temperature. Rubio et al. [9-11] have studied asymmetries in temperatures of water and glass cover, and amount of distillate for a double slope solar still (DSSS) by mathematical model (in terms of lumped parameters, and controlled temperatures of glass cover and basin). A correlation of mass transfer for condensing chamber of DSSS at different operating temperature ranges has been developed by Agrawal et al. [12]. Omri et al. [13] have examined the natural convection effects in solar stills for governing parameters such as Rayleigh number and tilt angle of glass cover. It has been shown that flow structure is sensitive to cover tilt angle. Dwivedi and Tiwari [14] have reported that DSSS produces daily yield 1.44 kg/m² at 'low production cost'. It has also been said that DSSS have energy efficiency 1.35% and energy pay back time

(EPBT) 1.6 years. A thermal model for DSSS and carbon credit earned by it, has been studied by Dwivedi and Tiwari [15]. Dwivedi and Tiwari [16] have developed a thermal model for double slope active solar still (DSASS). Cooper [17] has studied solar still's efficiency and suggested maximum efficiency can be as high as 60%. Tamimi [18] has characterized the characteristic curves of solar still between its ideal and the worst conditions. Boukar and Harmim [19] have obtained characteristic curve for vertical solar still and found its daily overall energy efficiency ranges from 7.9 to 21.2% under harsh condition of Sahara desert, Algeria. Tiwari and Noor [20] have presented the concept of an instantaneous thermal efficiency to characterize the solar stills. Dev and Tiwari [21-24] have developed the characteristic equation for single slope passive solar still, hybrid photovoltaic thermal (PVT) active solar still, double slope solar still and inverted absorber solar still at different water depths, inclinations and climatic conditions. Dev and Tiwari [21-24] have also reported that the non-linear characteristic curves are best fit to predict the behavior of solar stills. Dev et al. [23] have given characteristic equations for double slope solar still considering east and west sides of it separately which arose a need for a single characteristic equation for a single system instead of dividing a system into parts. A study of DSSS has been presented by Dwivedi [25]. Recently, a review on solar still have been done including various other water purification technologies e.g. membrane distillation [26]. Singh et al. [27] have experimentally studied the performance of hybrid PVT double slope active solar stills and found its daily average thermal efficiency 17.4% and highest yield 7.54 kg/day for parallel configuration of two flat plate collectors in forced mode of operation in October 2010 for composite climate of Ghaziabad, Uttar Pradesh, India. Dev [28] has studied various passive and active solar stills to develop their modified thermal models and characteristic equations. Dev and Tiwari [29] has recently studied the annual performance of evacuated tubular collector integrated single slope solar still to produce hot water along with distilled water (as a heat recovery from the evacuated tubular collector when water is stored at high temperatures).

Kumar and Agarwala [30] shown the energy computing models for optimally allocating different types of renewable in the distribution system for minimizing energy loss and optimizes the integration of renewable energy resources with technical and financial feasibility. Kamthania and Tiwari [31] shown the way to determine efficiency of semi transparent hybrid photovoltaic thermal double pass air collector for different PV technology and compare it with single pass air collector using artificial neural network (ANN) technique for New Delhi

¹Mechanical Engineering Department, Motilal Nehru National Institute of Technology Allahabad, Allahabad-211004, Uttar Pradesh, India.

²University Putra Malaysia, Dept. Civil Engineering, Faculty of Engineering, 43400 UPM Serdang, Selangor, Malaysia.

E-mail: ¹rahuldsurya@yahoo.com

weather station of India. Siddiqui et al. [32] developed efficiency metrics and time with efficiency relationship for the programmers and customers. Kumar et al. [33] describes energy efficient clustering for wireless sensor network with a large number of tiny sensor nodes to be used effectively in various applications with data accumulation. Kanchan and Kamthania [34] calculate the energy payback time for a building integrated semitransparent thermal (BISPVT) system with air duct. The work [30-34] shows broadly the calculation of efficiency with various parameters by software programmes including ANN, Matrices etc.

The objective of this paper is to obtain a new thermal model of DSSS (after assuming temperatures of both east and west side glass covers equal to their average temperature) and validating it by using experimental observations. The thermal model has been extended to obtain the expressions of daylight instantaneous gain and loss efficiencies of DSSS. Following these expressions, the characteristic curves of DSSS for its experimental performance under the composite climate of New Delhi, India, have been obtained and analyzed. The corresponding equations of these characteristic curves have been obtained and are to be used for thermal testing of DSSS for different climatic conditions, design parameters and materials.

2.0 EXPERIMENTAL SETUP AND OBSERVATIONS

A photograph of the experimental setup of DSSS is shown in Fig. 1. The experimental setup has been installed at Solar Energy Park, IIT Delhi, New Delhi, India. The orientation of the solar still has been kept east-west to receive solar radiation for maximum hours of sunshine and for increasing the heat addition into solar still. This affects the amounts of distillate on both sides of the solar still. The solar radiation incidents on both the glass covers and absorbed through the basin liner which heats the water. A small fraction of solar radiation is also absorbed by the glass covers and the water due to their absorptivities. The basin liner transfers the heat to the water through convection effect and also to the surroundings through the basin liner by conductive effect. The evaporated water from the basin comes in contact with the inner surfaces of the glass covers and releases its heat to the glass covers. The vapor again comes into the form of liquid water which trickles down to the troughs and then to the collecting jars placed at the east and west sides of the solar still. The glass takes the heat from the absorbed solar radiation and from the vapor which is released to the atmosphere by the wind through convection effect and radiation effect. In this phenomenon, two phase changes take places, (i) from basin water to vapor leaving impurities on the basin, and (ii) from vapor to water at the inner surface of glass covers. The amount of distillate depends upon the temperature difference between water and glass cover because of that it varies almost unequally at east and west sides of DSSS during daytime. When the sun lies in the east direction then higher temperature difference occur at west side due to low glass temperature which yields higher amount of distillate at this side and vice versa except at the time of noon when both the glass

covers have almost the same temperatures [14, 23, 25]. The distillate produced by the solar still has total dissolved solid count in the range of 8-15 ppm because some materials also evaporate within 0-100 °C and comes out with the distillate. The durations of sunshine hour at New Delhi are: 05:00-19:00 h (in summer); In winter this is 07:00-17:30 h (if no fog appears in the morning) or 9:00-17:30 h (if fog appears in the morning), with timings of solar noon in the respective month.



Figure 1: A photograph of double slope solar still.

DSSS has a box type structure of basin area 2 m². It has been made of the glass reinforced plastic (GRP) of thickness 5 mm painted black at inside surfaces to absorb the solar radiation. The heights of the solar still walls are 0.22 m at the east-west ends and 0.48 m at the center. Two simple window glasses of dimensions 1.03 × 1.06 × 0.004 m³ have been placed over the walls of the solar still at inclination angle 15°. The reasons of selecting this inclination angle are: (i) to receive maximum solar radiation when the sun is in the east or west direction, (ii) to guide condensed water into trough under the effects of forces namely adhesion force (between glass and water), cohesion force (between water molecules), and gravitational force, (iii) the minimum inclination angle can be chosen as $\{= \text{latitude of the place}(\phi_i) - 15^\circ\}$ for any solar still [28]. As the latitude of the place is 28°35' N for New Delhi, the angle of inclination can be equal to 13°35' which is taken as 15° (considering approximation) for the removing complexity and better understanding of the fabricator. An inlet has been provided through the north wall of the solar still to feed the brackish/saline water (i.e. total dissolved solids in the range of 1200 to 2000 parts per million as per availability in New Delhi). Two troughs have been fixed at inside surfaces of both the east and west walls of the solar still to collect the distilled water to guide the distillate into the collecting jar [14, 23, 25]. Figs. (2-5) show the various measured parameters on hourly basis for Dec'05 and Jun'06. Fig. 2 shows the hourly variations of incident solar radiation on both glass covers of DSSS.

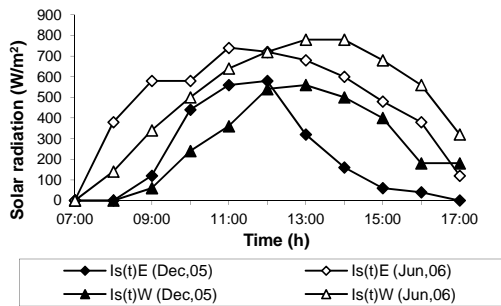


Figure 2: Hourly variations of solar radiation on both the east and west glass covers of DSSS on 9/12/2005 and 13/06/2006 [14, 23, 25].

Fig. 3 shows the hourly variations of water and ambient temperatures. Fig. 4 shows the hourly variations of temperatures of inner surface of both glass covers. Fig. 5 shows the hourly variations of distillate obtained from both sides of DSSS. Similar observations have been recorded for other months in duration from Oct'05 to Sep'06 [14, 15, 23, 25]. In Table 1, 'various design and operational parameters' and 'instruments used for measurements' have been given. Various parameters like temperatures, solar radiation and quantity of distillate on hourly basis have been measured for DSSS [25]. The annual experimental data (from Oct'05 to Sep'06) for DSSS taken at water depth of 0.01 m (i.e. 20 kg in DSSS) for New Delhi, India has been used to carry out the present analysis. The variations of incident total solar radiations (i.e. sum of direct and diffuse) on east and west glass covers for each month from Oct'05 to Sep'06 have been studied. It also shows that during noon hours the magnitudes of incident solar radiations are more or less same for both glass covers.

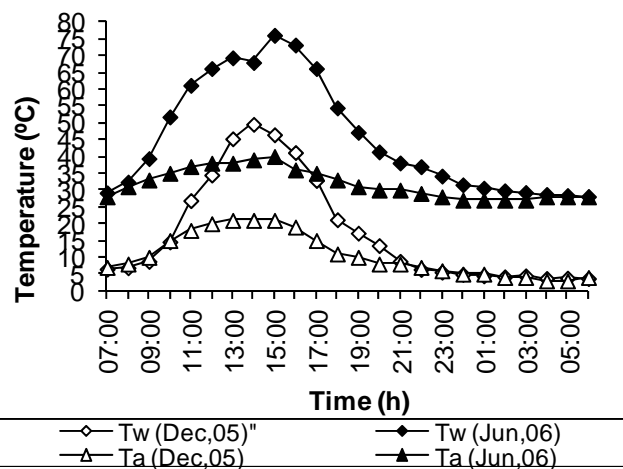


Figure 3: Hourly variations of water and ambient temperatures on 9/12/2005 and 13/06/2006 [14, 23, 25].

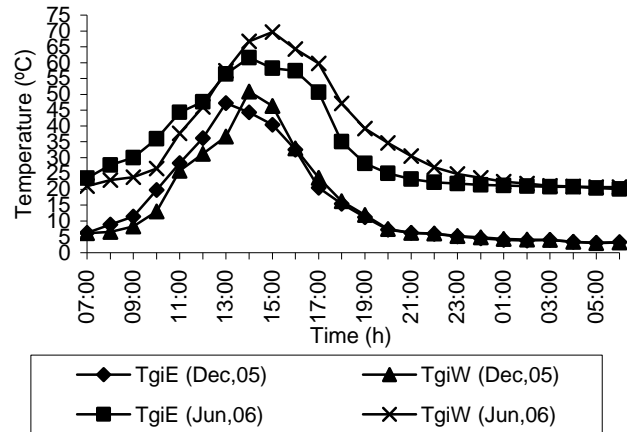


Figure 4: Hourly variations of temperatures of inner surfaces of both glass covers on 9/12/2005 and 13/06/2006 [14, 23, 25].

3.0 THERMAL MODEL

Following are the assumptions made for energy balance equations of different components of DSSS.

- i. DSSS is vapor leakage proof and is in quasi steady state.
- ii. There is no temperature gradient in the water inside the basin.
- iii. Heat capacities of glass and basin material are negligible.
- iv. Temperature dependant heat transfer coefficients have been considered.

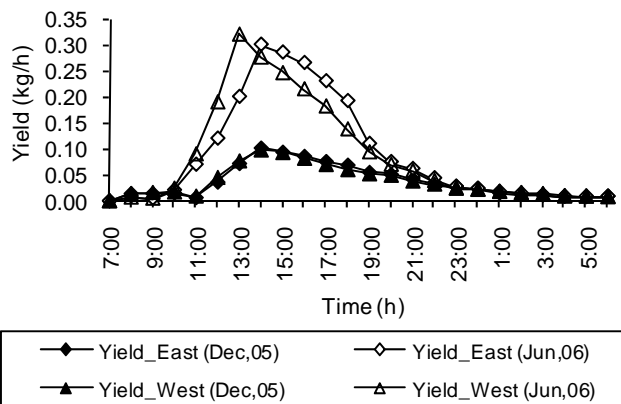


Figure 5: Hourly variations of distillate obtained from both sides of DSSS on 9/12/2005 and 13/06/2006 [14, 23, 25]. (a) Inner surface of east glass cover:

$$\left[\begin{array}{l} \text{Total energy absorbed} \\ \text{by inner surface} \\ \text{of east glass cover} \end{array} \right] = \left[\begin{array}{l} \text{Total energy released} \\ \text{by inner surface} \\ \text{of east glass cover} \end{array} \right]$$

i.e.

$$\left[\begin{array}{l} \text{Solar radiation} \\ \text{directly absorbed} \\ \text{glass cover} \end{array} \right] + \left[\begin{array}{l} \text{Heat energy released} \\ \text{from vapor to inner} \\ \text{surface of glass} \\ \text{cover} \end{array} \right] - \left[\begin{array}{l} \text{Heat energy} \\ \text{exchange} \\ \text{between both} \\ \text{glass covers} \end{array} \right]$$

$$= \left[\begin{array}{l} \text{Energy released} \\ \text{by inner surface} \\ \text{of east glass cover} \\ \text{to its outer surface} \end{array} \right]$$

$$\alpha'_g \cdot I_s(t)_E \cdot A_{gE} + h_{1wE} \cdot A_b \cdot (T_w - T_{giE}) - U_{EW} \cdot A_{gE} \cdot (T_{giE} - T_{giW}) = h_{kg} \cdot A_{gE} \cdot (T_{giE} - T_{goE}) \quad (1)$$

(b) Outer surface of east glass cover:

$$\left[\begin{array}{l} \text{Total energy absorbed} \\ \text{by outer surface} \\ \text{of east glass cover} \end{array} \right] = \left[\begin{array}{l} \text{Total energy released} \\ \text{by outer surface} \\ \text{of east glass cover} \\ \text{to ambient} \end{array} \right]$$

$$h_{kg} \cdot A_{gE} \cdot (T_{giE} - T_{goE}) = h_o \cdot A_{gE} \cdot (T_{goE} - T_a) \quad (2)$$

(c) Inner surface of west glass cover:

$$\left[\begin{array}{l} \text{Energy absorbed} \\ \text{by inner surface} \\ \text{of west glass cover} \end{array} \right] = \left[\begin{array}{l} \text{Energy released} \\ \text{by inner surface} \\ \text{of west glass cover} \end{array} \right]$$

i.e.

$$\left[\begin{array}{l} \text{Solar radiation} \\ \text{directly absorbed} \\ \text{glass cover} \end{array} \right] + \left[\begin{array}{l} \text{Heat energy released} \\ \text{from vapor to inner} \\ \text{surface of glass} \\ \text{cover} \end{array} \right] - \left[\begin{array}{l} \text{Heat energy} \\ \text{exchange} \\ \text{between both} \\ \text{glass covers} \end{array} \right]$$

$$= \left[\begin{array}{l} \text{Total energy released} \\ \text{by inner surface} \\ \text{of west glass cover} \\ \text{to its outer surface} \end{array} \right]$$

$$\alpha'_g \cdot I_s(t)_W \cdot A_{gW} + h_{1wW} \cdot A_b \cdot (T_w - T_{giW}) - U_{EW} \cdot A_{gW} \cdot (T_{giW} - T_{giE}) = h_{kg} \cdot A_{gW} \cdot (T_{giW} - T_{goW}) \quad (3)$$

(d) Outer surface of west glass cover:

$$\left[\begin{array}{l} \text{Total energy absorbed} \\ \text{by outer surface} \\ \text{of west glass cover} \end{array} \right] = \left[\begin{array}{l} \text{Total energy released} \\ \text{by outer surface} \\ \text{of west glass cover} \\ \text{to ambient} \end{array} \right]$$

$$h_{kg} \cdot A_{gW} \cdot (T_{giW} - T_{goW}) = h_o \cdot A_{gW} \cdot (T_{goW} - T_a) \quad (4)$$

(e) Basin liner:

$$\left[\begin{array}{l} \text{Total Energy} \\ \text{absorbed} \\ \text{by basin} \end{array} \right] = \left[\begin{array}{l} \text{Energy} \\ \text{released} \\ \text{by basin} \\ \text{to water} \end{array} \right] + \left[\begin{array}{l} \text{Energy released} \\ \text{by basin} \\ \text{to ambient} \end{array} \right]$$

$$\alpha'_b \cdot \{I_s(t)_E + I_s(t)_W\} \cdot A_b = h_{bw} \cdot A_b \cdot (T_b - T_w) + h_{ba} \cdot A_b \cdot (T_b - T_a) \quad (5)$$

(f) Water mass:

$$\left[\begin{array}{l} \text{Total Energy absorbed} \\ \text{by water i.e. from basin} \\ \text{and directly absorption of} \\ \text{solar radiation} \end{array} \right] = \left[\begin{array}{l} \text{Energy} \\ \text{stored in} \\ \text{water} \end{array} \right] + \left[\begin{array}{l} \text{Energy released} \\ \text{by water to inner} \\ \text{surfaces of east and} \\ \text{west glass covers} \end{array} \right]$$

$$+ \left[\begin{array}{l} \text{Energy released} \\ \text{by water to ambient} \\ \text{through side walls} \end{array} \right]$$

$$\alpha'_w \cdot \{I_s(t)_E + I_s(t)_W\} \cdot A_b + h_{bw} \cdot A_b \cdot (T_b - T_w) = (MC)_w \cdot \frac{dT_w}{dt} + h_{1wE} \cdot A_b \cdot (T_w - T_{giE}) + h_{1wW} \cdot A_b \cdot (T_w - T_{giW}) + h_s \cdot A_s \cdot (T_w - T_a) \quad (6)$$

Solving Eqs. (2) and (4), the following expressions have been obtained, temperatures of outer surface of east glass cover, of outer surface of west glass cover, inner surface of east glass cover, inner surface of west glass cover, basin:

$$T_{goE} = \frac{h_{kg} \cdot T_{giE} + h_o \cdot T_a}{h_{kg} + h_o} \quad (6a)$$

$$T_{goW} = \frac{h_{kg} \cdot T_{giW} + h_o \cdot T_a}{h_{kg} + h_o} \quad (6b)$$

$$T_{giE} = \frac{A_1 + A_2 \cdot T_w}{p} \quad (6c)$$

$$T_{giW} = \frac{B_1 + B_2 \cdot T_w}{p} \quad (6d)$$

$$T_b = \frac{\alpha'_b \cdot \{I_s(t)_E + I_s(t)_W\} + h_{bw} \cdot T_w + h_{ba} \cdot T_a}{h_{bw} + h_{ba}} \quad (6e)$$

Eq. (6) has been rearranged as follows,

$$\frac{dT_w}{dt} + aT_w = f(t) \quad (6f)$$

The following assumptions have also been made for solving Eq. (6f),

- i) Time interval dt ($0 < t < dt$).
- ii) Function $f(t) = \overline{f(t)}$ and a are constants for small interval dt .
- iii) Initial values of water and condensing cover temperatures have been used to determine the value of internal heat transfer coefficients.

Eq. (6f) has been solved to get following expression of water temperature T_w ,

$$T_w = \frac{\overline{f(t)}}{a} \cdot (1 - e^{-at}) + T_{w0} \cdot e^{-at} \quad (6g)$$

Expressions of $A_1, A_2, B_1, B_2, f(t)$ and a have been given in Appendix.

The rate of evaporative heat transfer for east and west side of the solar still can be written as,

$$\dot{q}_{ewE} = h_{ewE} (T_w - T_{giE}) \quad (6h)$$

$$\dot{q}_{ewW} = h_{ewW} (T_w - T_{giW}) \quad (6i)$$

$$\text{Substituting values of } T_{giE} \text{ and } T_{giW} \text{ in Eqs. (6h) and (6i) respectively, } \dot{q}_{ewE} = h_{ewE} \left\{ T_w - \left((A_1 + A_2 T_w) / p \right) \right\} \quad (6j)$$

or

$$\dot{q}_{ewE} = \frac{h_{ewE}}{p} \left\{ -\alpha'_g \cdot (I_s(t)_E h_{goW} + I_s(t)_E h_{1wW} + I_s(t)_E U_{EW} + I_s(t)_W U_{EW}) + (h_{goE} h_{goW} + h_{goE} h_{1wW} + h_{goE} U_{EW} + h_{goW} U_{EW}) \cdot (T_w - T_a) \right\} \quad (6k)$$

$$\text{and} \quad \dot{q}_{ewW} = h_{ewW} \left\{ T_w - \left((B_1 + B_2 T_w) / p \right) \right\} \quad (6l)$$

$$\text{or} \quad \dot{q}_{ewW} = \frac{h_{ewW}}{p} \left\{ -\alpha'_g \cdot (I_s(t)_E U_{EW} + I_s(t)_W h_{goE} + I_s(t)_W h_{1wE} + I_s(t)_W U_{EW}) + \left(h_{goE} U_{EW} + h_{goE} h_{goW} + h_{goW} h_{1wE} + h_{goW} U_{EW} \right) \cdot (T_w - T_a) \right\} \quad (6m)$$

Eqs. (6k) and (6m) can be added to get the rate of total evaporative heat transfer by making some additional assumptions for a different approach of thermal modeling of DSSS. These assumptions are as follows:

- v) Areas of both glass covers are 1 m^2 .

$$\text{vi) Temperatures of both glass covers are equal to their average temperature } (T_{giEW}) \text{ i.e. } T_{giEW} = (T_{giE} + T_{giW}) / 2 \quad (6n)$$

Then the temperature difference between water and glass cover temperatures become $(T_w - T_{giEW})$. Due to which various internal heat transfers of both sides from water to glass covers become equal. Convective, radiative and evaporative heat transfer coefficients from water to east and west side glass covers can be written as:

$$h_{cwE} = h_{cwW} \quad ; \quad h_{rwE} = h_{rwW} \quad ; \quad h_{ewE} = h_{ewW} \text{ which results } h_{1wE} = h_{1wW} = h_{1wEW} \quad (6o)$$

- vii) the total (radiative and convective) heat transfer coefficients from both glass covers to ambient air become equal as these terms depends upon wind velocity (Eqs. 1-4) i.e. $h_o = 5.7 + 3.8v = h_{oEW}$ (6p)

And, therefore, the heat transfer coefficients from inner surfaces of glass covers to ambient air also become equal and can be represented by following expressions,

$$h_{goE} = h_{goW} = h_{goEW} \quad (6q)$$

where,

$$h_{goE} = h_{goW} = \frac{h_{kg} \cdot h_o}{h_{kg} + h_o},$$

From Eqs. (1-6), Eqs. (6n - 6q) and assumptions similar to solve Eq. (6f), the following expression of water temperature can be obtained as,

$$T_{wEW} = \frac{\overline{f(t)}_{EW}}{a_{EW}} \left[1 - e^{-a\Delta t} \right] + T_{w0} e^{-a\Delta t} \quad (7)$$

$$\text{where, } a_{EW} = \frac{1}{(MC)_w} \left[\frac{2h_{bw}h_{ba}}{h_{bw} + h_{ba}} + \frac{h_{1wEW}}{p_{EW}} \left\{ 2h_{goEW}^2 + 4h_{goEW}U_{EW} + 2h_{goEW}h_{1wEW} \right\} \right];$$

$$p_{EW} = (h_{goEW}^2 + h_{1wEW}^2 + 2h_{goEW}U_{EW} + 2h_{1wEW}h_{goEW} + 2h_{1wEW}U_{EW})$$

$$f(t)_{EW} = \frac{1}{(MC)_w} \left[\left(\alpha'_w + \frac{\alpha'_b h_{bw}}{h_{bw} + h_{ba}} \right) (I_s(t)_E + I_s(t)_w) + \frac{h_{1wEW}}{P_{EW}} \left\{ \begin{aligned} & \left(\alpha'_g h_{1wEW} + h_{goEW} + 2U_{EW} \right) (I_s(t)_E + I_s(t)_w) \\ & + T_a \left(2h_{goEW} h_{1wEW} + 2h_{goEW}^2 + 4h_{goEW} U_{EW} \right) \end{aligned} \right\} \right. \\ \left. + \left(\frac{2h_{bw} h_{ba}}{h_{bw} + h_{ba}} \right) T_a \right]$$

Adding Eqs. (6k) and (6m), the expression of combined rate of evaporative heat transfer from water to both glass covers can be written as

$$\dot{q}_{ewEW} = \frac{h_{ewEW}}{P_{EW}} (I_s(t)_E + I_s(t)_W) \left\{ -\alpha'_g \cdot (2U_{EW} + h_{goEW} + h_{1wEW}) + \right. \\ \left. \left(2h_{goEW}^2 + 4h_{goEW} U_{EW} + 2h_{goEW} h_{1wEW} \right) (T_{wEW} - T_a) / (I_s(t)_E + I_s(t)_W) \right\} \tag{8}$$

Further, the following linear expression of daylight instantaneous gain efficiency of DSSS $\left(\eta_i = \frac{\text{Heat output in the form of distilled water per unit time}}{\text{Total heat input in the system per unit time}} = \text{denoted as } y_1 \text{ also} \right)$ has been obtained by using Eq. (7).

$$\eta_{iEW} = \frac{\dot{q}_{ewEW}}{(I_s(t)_E \cdot A_{gE} + I_s(t)_W \cdot A_{gW})} = (\alpha\tau)_{eff1} + (UA)_{eff1} \cdot \left\{ (T_{wEW} - T_a) / (I_s(t)_E + I_s(t)_W) \right\} \tag{9}$$

where, $(\alpha\tau)_{eff1} = -\alpha'_g \cdot (h_{goEW} + 2U_{EW} + h_{1wEW}) \cdot \frac{h_{ewEW}}{P_{EW}}$; $(UA)_{eff1} = 2(h_{goEW}^2 + 2h_{goEW} U_{EW} + h_{goEW} h_{1wEW}) \cdot \frac{h_{ewEW}}{P_{EW}}$;

Similarly, an expression for the daylight instantaneous loss efficiency (i.e. efficiency due to heat storage effect of water

$\left(\eta_i = \frac{\text{Heat stored in the water per unit time}}{\text{Total heat input in the system per unit time}} = \text{denoted as } y_2 \text{ also} \right)$ can be given as,

$$\eta_{iLEW} = \frac{(MC)_w \times (T_{wEW} - T_{wo})}{(I_s(t)_E \cdot A_{gE} + I_s(t)_W \cdot A_{gW})} = (\alpha\tau)_{eff2} - (UA)_{eff2} \cdot \frac{(T_{wEW} - T_a)}{(I_s(t)_E + I_s(t)_W)} \tag{10}$$

Eq. (10) is also a linear characteristic equation.

where, $(\alpha\tau)_{eff2} = \frac{(MC)_w (1 - e^{-a\Delta t}) \left\{ \alpha'_w + \frac{\alpha'_b h_{bw}}{h_{bw} + h_{ba}} + \frac{h_{1wEW}}{P_{EW}} \left(\alpha'_g h_{1wEW} + h_{goEW} + 2U_{EW} \right) \right\}}{\left\{ \frac{2h_{bw} h_{ba}}{h_{bw} + h_{ba}} + \frac{h_{1wEW}}{P_{EW}} \left(2h_{goEW}^2 + 4h_{goEW} U_{EW} + 2h_{goEW} h_{1wEW} \right) \right\}}$

and $(UA)_{eff2} = (MC)_w (1 - e^{-a\Delta t})$ are heat gain and heat loss terms respectively.

Location	Solar Energy Park, I.I.T. Delhi	Quantity of glass	2
Specification of the location	28°35' N, 77°12' E, altitude 216 m from mean sea level	Inclination angle	15°
Climate	Composite	Color of walls inside	Black
Orientation	East - West	No of inlet to saline water	1
Body material	Glass reinforced plastic (GRP)	No of outlet connected with trough at ends	2
Basin area	2 m ²	Water depth	0.01 m
Thickness of GRP	0.005 m	Latent heat of vaporization (L)	2390 × 10 ³ J/kg
Height at ends	0.22 m	Specific heat of water (C _w)	4200 J/kgK
Height at centre	0.48 m	Mass of water (M)	20 kg
Simple window glass	1.03 × 1.06 × 0.004 m ³	Wind velocity (v)	4.5 m/s
K _b	0.0351 W/mK	α' _w	0.5
K _g	0.78 W/mK	ε _g	0.9
α' _b	0.7	ε _w	0.9
α' _g	0.2	ε _{eff}	0.82
U _{bw}	300 W/m K		
Calibrated Thermocouples	copper-constantan (T type) measuring range -200 to 350 °C and sensitivity of 43 μV/°C		
Digital temperature indicator	resolution 0.1°C, range -20 to 450 °C		
Solarimeter	resolution 20 W/m ² , range 0-1200 W/m ²		
Calibrated mercury thermometer	resolution 1°C, range 0-120 °C		
Measuring jar	resolution 10 ml, range 0-100 ml		

Table 1: Design and operational parameters of DSPSS, and description of measuring instruments.

4.0 RESULTS AND DISCUSSION

Fig. 6 shows the comparison of previous (Eq. (6g)) and new thermal model (Eq. (7)) with experimental observations of DSSS for the month of June (date: 13/06/06). A close agreement have been found for both thermal models (previous thermal model and new thermal model with RMS errors 10.08% and 10.12% respectively with experimental results) for a given design and operational parameters (Table 1) over 24 h with experimental values. The RMS errors are at higher sides due to several assumptions and heat losses but with similar variation as experimental values have. Figs. 7 and 8 show the hourly variations of experimental and theoretical values of various temperatures, and amount of distillate respectively obtained in duration 7:00 h to 17:00 h for DSSS at water depth 0.01 m for the month of June'06. A fair agreement in temperature of water with root mean percentage square (RMS) error 6.8% (coefficient of correlation r=0.9671) has been found. Similarly, RMS error for total amount of yield obtained experimentally and theoretically from both east and west sides of DSSS has been found 34.7% with r=0.9753, as shown in Fig. 8.

Further for plotting the characteristic curves based on Eqs. (9) and (10), average values of various temperatures, solar radiation and yield for any time (e.g. 10:00 h) over a year considering all months have been calculated. Variable nature of climatic parameters (which are non-linear in nature) like solar

intensity, ambient temperature and wind speed give results unrealistic values of instantaneous gain/loss efficiencies such as $\eta_i, \eta_{iL} > 1$ and $\eta_i, \eta_{iL} < 0$ especially for low solar intensities, low water temperature in the morning and cooling of water takes place in the evening to next day's morning. Hence, the quasi steady state for DSSS has been taken during the mid-day sunshine hours only i.e. 10:00 h to 14:00 h [21-24]. It is a high solar intensity period in which the 'average value of solar radiation' can be seen nearly equal to the 'hourly variation of solar radiation of the period'.

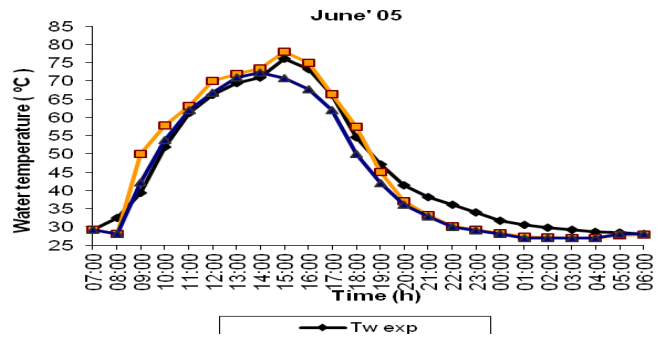


Figure 6: Comparison of old and new thermal model with experimental observations of DSSS for the month of June (date: 13/06/06).

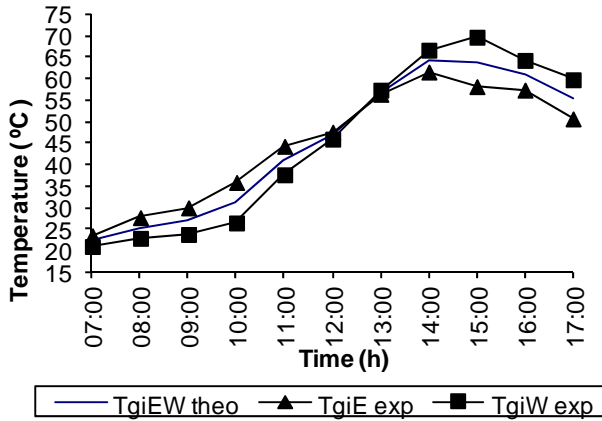


Figure 7: Variation of theoretical and experimental values of temperatures of inner surfaces of both glass covers for the month of June (date: 13/06/06).

Figs. 9 and 10 show linear and non-linear characteristics with their equations for DSSS for the month of Dec'05. The valid range of $x = \left\{ \frac{(T_{wEW} - T_a)}{(I_s(t)_E + I_s(t)_W)} \right\}$ including threshold and maximum values has been found $0.0069 \leq x \leq 0.0645$ from the Figs. 9 and 10. Similarly, linear and non-linear characteristics with their equations for DSSS have been obtained for the month of Jun'06. The valid range of x including threshold and maximum values has been found $0.0137 \leq x \leq 0.0229$. Following are the instantaneous gain and loss efficiency equations obtained for the month of June'06.

for instantaneous gain efficiency: $y_{1exp} = 18.348x - 0.2785$ for ($R^2 = 0.983$, $RMS_e = 45.4$, $x_{thr} = 0.0152$)

$y_{1exp} = 1226.2x^2 - 28.355x + 0.1582$ for ($R^2 = 0.9989$, $RMS_e = 1.6$, $x_{thr} = 0.0137$)

for instantaneous loss efficiency: $y_{1exp} = -16.338x - 0.3933$ for ($R^2 = 0.9175$, $RMS_e = 30.4$, $x_{thr} = 0.0241$)

$y_{1exp} = -2331.2x^2 - 72.45x - 0.4369$ for ($R^2 = 0.9848$, $RMS_e = 15.8$, $x_{thr} = 0.0229$)

The linear and non-linear characteristic curves based on an annual experimental performance of DSSS has been analyzed. The corresponding equations of these characteristic curves are given as follows, for instantaneous gain efficiency: $y_{1exp} = 19.621x - 0.1458$ for ($R^2 = 0.9856$, $RMS_e = 25.6$, $x_{thr} = 0.0074$) & $y_{1exp} = 18.26x^2 + 19.048x - 0.1418$ for ($R^2 = 0.9857$, $RMS_e = 24.1$, $x_{thr} = 0.0074$)

for instantaneous loss efficiency: $y_{1exp} = -12.478x + 0.3392$ for ($R^2 = 0.8591$, $RMS_e = 15.5$, $x_{thr} = 0.0272$) &

$y_{1exp} = 1013.3x^2 - 44.278x + 0.5617$ for ($R^2 = 0.9925$, $RMS_e = 5.4$, $x_{thr} = 0.0218$)

The valid range of x for linear characteristic curves (including both instantaneous gain and loss efficiency curves) is found to be $0.0074 \leq x \leq 0.0272$ °C/W-m². Similarly, for non-linear characteristic curves the valid range of x is found to be $0.0074 \leq x \leq 0.0218$ °C/W-m².

Considering, all linear and non-linear characteristic curves of DSSS, the actual valid range of x is established as $0.0069 \leq x \leq 0.0229$ °C/W-m². It is seen that non-linear characteristic curves have lower values of RMS errors with higher values of

coefficient of determination (R^2) to their corresponding linear characteristic curves. Both 'RMS error' and 'coefficient of determination' are subjected to various parameters (climatic, operational and design) and procedure of measurement (i.e. time interval between two consecutive measurements) in case of solar stills. It can be concluded that to increase the accuracies of characteristic equations, it is required to reduce the heat loss, vapor loss by using appropriate materials for insulation and packing respectively, and also the time interval between two consecutive observations. On the basis of these observations, non-linear characteristic curves (due to higher accuracy) are found better analytical tools for thermal testing of DSSS for different materials, operational and climatic parameters. In other words, it is because solar stills can be made of fiber reinforced plastic/glass reinforced plastic, Galvanized iron sheet with proper insulation, wood, concrete etc. All these materials have different thermal conductivities and material thickness

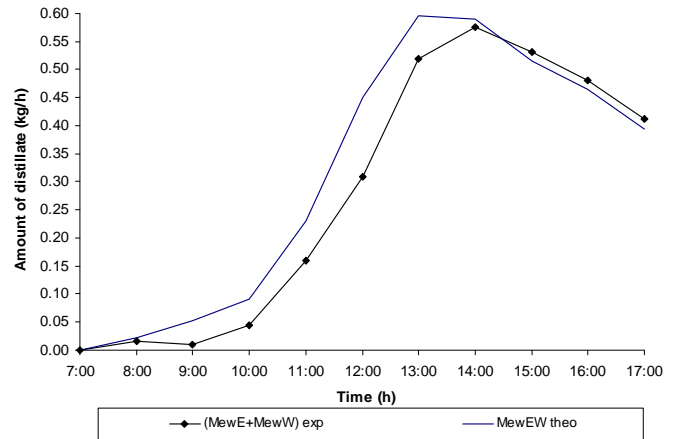


Figure 8: Theoretical and experimental variations of total amount of distillate collected from east and west sides of DSSS for the month of June (date: 13/06/06).

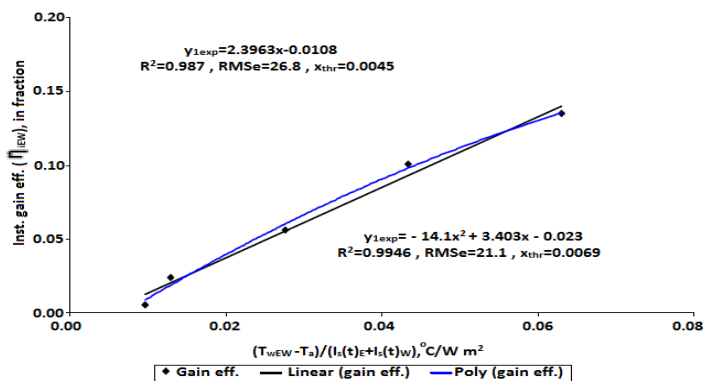


Figure 9: Linear and non-linear gain characteristic curves for DSSS for the month of Dec'05.

Hence, on the basis of use of different materials different characteristics of DSSS can also be obtained and compared for better material and its thickness with optimized cost of fabrication (the cost of fabrication is dependent upon material).

Similarly, operational parameters such as water depth, salinity would also give different characteristics of DSSS which can be compared to get optimized operational parameters. The climatic parameters depend upon the latitude of the place. Hence, for different locations different characteristics can be obtained. The established results for characteristic equations of DSSS is similar to previously established results for single slope solar still [21], hybrid (PV-T) active solar still [22], double slope solar still [23], and inverted absorber solar still [24].

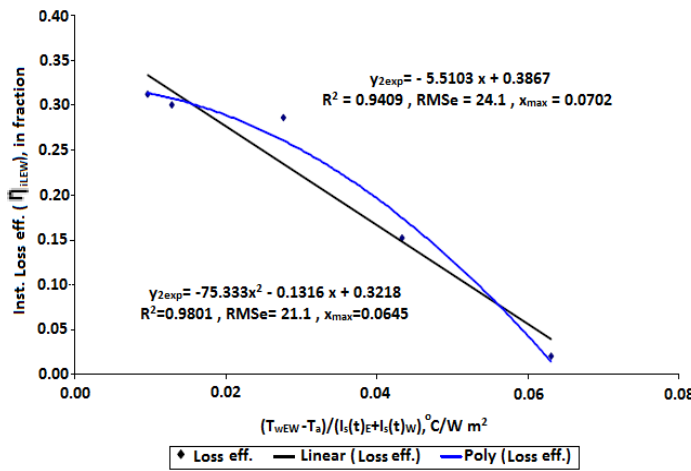


Figure 10: Linear and non-linear loss characteristic curves for DSSS for the month of Dec'05.

CONCLUSIONS

On the basis of above analysis, the new thermal model of DSSS (developed after considering temperatures of east and west side glass covers equal to their average temperature) has been found in fair agreement with experimental observations. Further, the characteristic equations based on the thermal model and experimental data have been obtained. Non-linear characteristic curves have been found more accurate for DSSS in comparison to its linear characteristic curves.

NOMENCLATURE

- A_b Area of the basin (m^2)
- A_{gE} Area of the east side glass cover (m^2)
- A_{gW} Area of the west side glass cover (m^2)
- C specific heat of water ($J/Kg\ ^\circ C$)
- dt Small time interval (s)
- $\frac{dT_w}{dt}$ Change in water temperature in small time dt ($^\circ C/s$)
- h_{ba} Conductive heat transfer coefficient from basin to ambient ($W/m^2\ ^\circ C$)
- h_{bw} Convective heat transfer coefficient from basin to water ($W/m^2\ ^\circ C$)
- h_{goE} Combined convective and radiative heat transfer coefficient from inner surface of east glass cover to ambient ($W/m^2\ ^\circ C$)

- h_{goEW} Combined convective and radiative heat transfer coefficient from inner surfaces of glass covers to ambient ($W/m^2\ ^\circ C$)
- h_{gow} Combined convective and radiative heat transfer coefficient from inner surface of west glass cover to ambient ($W/m^2\ ^\circ C$)
- h_{kg} Conductive heat transfer coefficient of glass cover ($W/m^2\ ^\circ C$)
- h_s Heat transfer coefficient of side wall ($W/m^2\ ^\circ C$)
- h_o total convective and radiative heat transfer coefficient from east/west side glass cover to ambient ($W/m^2\ ^\circ C$)
- h_{oEW} total convective and radiative heat transfer coefficient from either east or west side glass cover to ambient ($W/m^2\ ^\circ C$)
- $I_s(t)_W$ solar intensity incident on the west side glass cover (W/m^2)
- K_g thermal conductivity of glass covers ($W/m\ K$)
- L_g thickness of glass covers (m)
- L latent heat of vaporization (J/kg)
- M mass of water in the basin of solar still (kg)
- P_w partial saturated vapor pressure at water temperature (N/m^2)
- P_{gi} partial saturated vapor pressure at inner glass temperature (N/m^2)
- \dot{q}_{ewEW} Total evaporative heat gain (W)
- T_a ambient air temperature ($^\circ C$)
- T_b basin temperature ($^\circ C$)
- T_{giE} inner glass covers temperature on east side ($^\circ C$)
- T_{giW} inner glass covers temperature on west side ($^\circ C$)
- T_{giEW} Average temperature of inner surfaces of glass covers of DSSS ($^\circ C$)
- T_{goE} outer glass covers temperature on east side ($^\circ C$)
- T_{gow} outer glass covers temperature on west side ($^\circ C$)
- T_w water temperature ($^\circ C$)
- T_{wo} water temperature at time $t=0$ ($^\circ C$)
- T_{wEW} Water temperature after assumption of average glass cover temperature ($^\circ C$)
- U_{EW} radiative heat transfer coefficient between east and west glass cover ($W/m^2\ ^\circ C$)
- v wind velocity (m/s)
- α'_b Solar flux absorption factor for basin liner
- α'_g Solar flux absorption factor for glass
- α'_w Solar flux absorption factor for water
- α_{eff} Effective absorptivity of the whole solar still assembly
- ϵ_{eff} Effective emissivity
- ϵ_g Emissivity of glass cover
- ϵ_w Emissivity of water
- σ Stephan-Boltzman constant ($W/m^2\ K^4$)
- η_{iEW} Instantaneous gain efficiency (γ_1)
- η_{iLEW} Instantaneous loss efficiency (γ_2)

h_{IwE}	total internal heat transfer coefficient from water to glass cover on east side ($W/m^2\text{ }^\circ C$)
h_{IwW}	total internal heat transfer coefficient from water to glass cover on west side ($W/m^2\text{ }^\circ C$)
h_{cwE}	internal convective heat transfer coefficient from water to glass cover on east side ($W/m^2\text{ }^\circ C$)
h_{cwEW}	internal convective heat transfer coefficient from water to both glass covers ($W/m^2\text{ }^\circ C$)
h_{cwW}	internal convective heat transfer coefficient from water to glass cover on west side ($W/m^2\text{ }^\circ C$)
h_{ewE}	internal evaporative heat transfer coefficient from water to glass cover on east side ($W/m^2\text{ }^\circ C$)
h_{ewEW}	internal evaporative heat transfer coefficient from water to both glass covers ($W/m^2\text{ }^\circ C$)
h_{ewW}	internal evaporative heat transfer coefficient from water to glass cover on west side ($W/m^2\text{ }^\circ C$)
h_{rwE}	internal radiative heat transfer coefficient from water to glass cover on east side ($W/m^2\text{ }^\circ C$)
h_{rwEW}	internal radiative heat transfer coefficient from water to both glass covers ($W/m^2\text{ }^\circ C$)
h_{rwW}	internal radiative heat transfer coefficient from water to glass cover on west side ($W/m^2\text{ }^\circ C$)
$I_s(t)_E$	solar intensity incident on the east side glass cover (W/m^2)
$I_s(t)_{EW}$	Total solar intensity on both glass covers ($I_s(t)_{EW} = I_s(t)_E + I_s(t)_W$, W/m^2)

REFERENCES

[1]. G.N. Tiwari, A.K. Tiwari, Solar distillation practice for water desalination systems. Anamaya Publishers, New Delhi, India, 2007.

[2]. A. Kaushal, Varun, Solar stills: A review, *Renew. Sust. Ener. Rev.* 14 (2010) 446-453.

[3]. G.N. Tiwari, H.N. Singh, R. Tripathi, Present status of solar distillation, *Sol. Ener.* 75 (2003) 367-73.

[4]. M.A.S. Malik, G.N. Tiwari, A. Kumar, M.S. Sodha, Solar distillation, Pergamon Press, Oxford, UK 1982.

[5]. G. Nebbia, G. Menozzi, *Acque Dolce Dal Mare*, 11 *Inchiesta Inter. Milano.* 1966; 129-172.

[6]. G.B. Della Porta, *Magiae naturalis libri XX.* Napoli. 1589.

[7]. R.V. Dunkle, Solar water distillation: The roof type still and multiple effect diffusion solar still, *Int. Dev. Heat Trans.*, ASME proceedings, (part 5): 895-902, 1961.

[8]. P.T. Tsilingiris, Modeling heat and mass transport phenomena at higher temperatures in solar distillation systems-The Chilton-Colburn analogy, *Sol. Ener.* 84 (2010) 308-317.

[9]. E. Rubio, J.L. Fernandez, M.A. Porta-Gandara, Modeling thermal asymmetries in double slope solar stills, *Renew. Ener.* 29 (2004) 895-906.

[10]. E. Rubio, M.A. Porta, J.L. Fernandez, Cavity geometry influence on mass flow rate for single and double slope solar stills, *Appl. Ther. Engg.* 20 (2000) 1105-1111.

[11]. E. Rubio-Cerda, M.A.P. Gandara, J.L.F. Zayas, Thermal performance of the condensing covers in a triangular solar still, *Renew. Ener.* 27 (2002) 301-308.

[12]. S. Agrawal, G.N. Tiwari, Thermal modeling of a double condensing chamber solar still: an experimental validation, *Ener. Conver. Manage.* 40 (1999) 97-114.

[13]. A. Omri, J. Orfi, S.B. Nasrallah, Natural convection effects in solar stills, *Desalination* 183 (2005) 173-178.

[14]. V.K. Dwivedi, G.N. Tiwari, Annual energy and exergy analysis of single and double slope passive solar stills, *Appl. Sci. Res.* 3(3) (2008) 225-241.

[15]. V.K. Dwivedi, G.N. Tiwari, Thermal modeling and carbon credit earned of a double slope passive solar still, *Desalination and Water Treatment* 13 (2010) 400-410.

[16]. V.K. Dwivedi, G.N. Tiwari, Experimental validation of thermal model of a double slope active solar still under natural circulation mode, *Desalination* 250 (2010) 49-55.

[17]. P.I. Cooper, Maximum efficiency of a single effect solar still, *Sol. Ener.* 15 (1973) 205-214.

[18]. A. Tamimi, Performance of a solar still with reflectors and black dye, *Solar & Wind Technology* 4 (1987) 443-446.

[19]. M. Boukar, A. Hramim, Performance evaluation of a one-sided vertical solar still tested in the desert of Algeria, *Desalination* 183 (2005) 113-126.

[20]. G.N. Tiwari, M.A. Noor, Characterisation of solar stills, *Sol. Ener.* 18 (1996) 147-171.

[21]. R. Dev, G.N. Tiwari, Characteristic equation of single slope passive solar still, *Desalination* 245 (2009) 246-265.

[22]. R. Dev, G.N. Tiwari, Characteristic equation of hybrid (PV-T) active solar still, *Desalination* 254 (2010) 126-137.

[23]. R. Dev, H.N. Singh, G.N. Tiwari, Characteristic equation of double slope passive solar still, *Desalination* 267 (2011) 261-266.

[24]. R. Dev, G.N. Tiwari, Characteristic equation of the inverted absorber solar still, *Desalination* 269 (2010) 67-77.

[25]. V.K. Dwivedi, Performance study of various designs of solar still, PhD Thesis, Centre for Energy Studies, IIT Delhi, New Delhi, India (2008) 67-91.

[26]. R. Dev, G.N. Tiwari, Chap-6: Solar Distillation, In: C. Ray, R. Jain editors, *Drinking Water Treatment: Focusing on Appropriate Technology and Sustainability*, Springer, New York 1st ed. (2011) 159-210.

[27]. G. Singh, S. Kumar, G.N. Tiwari, Design, fabrication and performance evaluation of a hybrid photovoltaic thermal (PVT) double slope active solar still, *Desalination* 277 (2011) 399-406.

[28]. R. Dev, Thermal modeling and characteristic equations for passive and active solar stills, PhD Thesis, Centre for Energy Studies, IIT Delhi, New Delhi, India (2012) 23-24.

[29]. R. Dev, G.N. Tiwari, Annual performance of evacuated tubular collector integrated single slope solar still, *Desalination and Water Treatment*, 41 (2012) 204-223.

[30]. R. Kumar, A. Agarwala, Survey of Energy Computing in the Smart Grid Domain, *BIJIT - BVICAM's International Journal of Information Technology*, 5 (1) (2013) 525-530.

- [31]. D. Kamthania, G. N. Tiwari, Determination of Efficiency of Hybrid Photovoltaic Thermal Air Collectors using Artificial Neural Network Approach for Different PV Technology, BIJIT, 4 (1) (2012) 397-404.
- [32]. T. Siddiqui, M. A. Wani, N. A. Khan, Efficiency Metrics, BIJIT, 3 (2) (2011) 377-381.
- [33]. D. Kumar, T. C. Aseri, R. B. Patel, EECHDA: Energy Efficient Clustering Hierarchy and Data Accumulation For Sensor Networks, BIJIT, 2(1) (2010) 150-157.
- [34]. K. Mudgil, D. Kamthania, Energy Payback Time Calculation for a Building Integrated Semitransparent Thermal (BISPVT) System with Air Duct, BIJIT, 5 (2) (2013) 593-596.

APPENDIX [7, 14, 25]

solar flux absorption factor for glass $\alpha'_g = (1 - R_g)\alpha_g$; for water $\alpha'_w = (1 - \alpha_g)(1 - R_g)(1 - R_w)\alpha_w$;

for basin liner $\alpha'_b = \alpha_b(1 - \alpha_g)(1 - R_g)(1 - R_w)(1 - \alpha_w)$; and $\varepsilon_{eff} = \left[\left(\frac{1}{\varepsilon_g} \right) + \left(\frac{1}{\varepsilon_w} \right) - 1 \right]^{-1}$; $h_o = 5.7 + 3.8v$; $h_{kg} = k_g / l_g$; $h_b = k_b / l_b$;

$$h_{rwE} = \varepsilon_{eff} \cdot \sigma \left[(T_w + 273)^2 + (T_{giE} + 273)^2 \right] \left[T_w + T_{giE} + 546 \right]; h_{rwW} = \varepsilon_{eff} \cdot \sigma \left[(T_w + 273)^2 + (T_{giW} + 273)^2 \right] \left[T_w + T_{giW} + 546 \right];$$

$$h_{goE} = \left[(1/h_{kg}) + (1/h_o) \right]^{-1} = h_{goW}; h_{ba} = \left[(1/h_b) + (1/h_o) \right]^{-1}; h_{cwE} = 0.884 \left[(T_w - T_{giE}) + (P_w - P_{giE})(T_w + 273) / (268.9 \times 10^3 - P_w) \right]^{1/3};$$

$$P_w = \exp \left[25.317 - (5144 / (T_w + 273.15)) \right]; h_{cwW} = 0.884 \left[(T_w - T_{giW}) + \frac{(P_w - P_{giW})(T_w + 273)}{268.9 \times 10^3 - P_w} \right]^{1/3}; h_{ewE} = 16.273 \times 10^{-3} \times h_{cwE} \times \frac{(P_w - P_{giE})}{(T_w - T_{giE})};$$

$$h_{ewW} = 16.273 \times 10^{-3} \times h_{cwW} \times \frac{(P_w - P_{giW})}{(T_w - T_{giW})}; P_{giE} = \exp \left[25.317 - (5144 / (T_{giE} + 273.15)) \right]; P_{giW} = \exp \left[25.317 - (5144 / (T_{giW} + 273.15)) \right];$$

$$h_{1wE} = h_{cwE} + h_{rwE} + h_{ewE}; h_{1wW} = h_{cwW} + h_{rwW} + h_{ewW}; U_1 = h_{1wE}A_b + U_{EW}A_{gE} + h_{go}A_{gE}; U_2 = h_{1wW}A_b + U_{EW}A_{gW} + h_{go}A_{gW}$$

$$R_1 = \alpha'_g I_s(t)_E A_{gE} + h_{go}A_{gE}T_a + h_{1wE}A_bT_w; R_2 = \alpha'_g I_s(t)_W A_{gW} + h_{go}A_{gW}T_a + h_{1wW}A_bT_w; A_1 = R_1 U_2 + R_2 U_{EW} A_{gE};$$

$$B_1 = R_1 U_{EW} A_{gW} + R_2 U_1; A_2 = h_{1wE} A_b U_2 + h_{1wW} A_b U_{EW} A_{gE}; B_2 = h_{1wE} A_b U_{EW} A_{gW} + h_{1wW} A_b U_1; p = U_1 U_2 - U_{EW} A_{gE} A_{gW}$$

$$U_{EW} = 0.034 \sigma \left[(T_{giE} + 273)^2 + (T_{giW} + 273)^2 \right] \left[T_{giE} + T_{giW} + 546 \right]; (T_w - T_{giE}) = ((p - A_2)T_w - A_1) / p; (T_w - T_{giW}) = ((p - B_2)T_w - B_1) / p$$

$$(T_b - T_w) = \left(\alpha'_b \{ I_s(t)_E + I_s(t)_W \} + h_{ba} T_a - h_{ba} T_w \right) / (h_{bw} + h_{ba}); a = \left\{ \frac{h_{bw} h_{ba} A_b + h_{1wE} (p - A_2) A_b + h_{1wW} (p - B_2) A_b + h_{sw} A_{sw}}{h_{bw} + h_{ba}} \right\} / (MC)_w$$

$$f(t) = \left[\left\{ \frac{\alpha'_b h_{bw}}{h_{bw} + h_{ba}} \right\} A_b (I_s(t)_E + I_s(t)_W) + \left\{ \frac{h_{bw} h_{ba} A_b + h_{sw} A_{sw}}{h_{bw} + h_{ba}} \right\} T_a + \left\{ \frac{(h_{1wE} A_1 + h_{1wW} B_1) A_b}{p} \right\} \right] / (MC)_w;$$

After assuming $\rightarrow T_{giE} = T_{giW} = (T_{giE} + T_{giW}) / 2 = T_{giEW}$; $h_{rwEW} = \varepsilon_{eff} \cdot \sigma \left[(T_w + 273)^2 + (T_{giEW} + 273)^2 \right] \left[T_w + T_{giEW} + 546 \right];$

$$h_{cwEW} = 0.884 \left[(T_w - T_{giEW}) + (P_w - P_{giEW})(T_w + 273) / (268.9 \times 10^3 - P_w) \right]^{1/3}; h_{ewEW} = 16.273 \times 10^{-3} \times h_{cwEW} \times (P_w - P_{giEW}) / (T_w - T_{giEW});$$

$$P_{giEW} = \exp \left[25.317 - (5144 / (T_{giEW} + 273.15)) \right]; P_w = \exp \left[25.317 - (5144 / (T_w + 273.15)) \right]; h_{1wEW} = h_{rwEW} + h_{cwEW} + h_{ewEW}$$